applied sciences

MDPI

Article

Carbon Nano-Onion Peroxidase Composite Biosensor for Electrochemical Detection of 2,4-D and 2,4,5-T

Vibol Sok and Alex Fragoso *

Departament d'Enginyeria Química, Universitat Rovira i Virgili, 43007 Tarragona, Spain; vibol.sok@urv.cat
* Correspondence: alex.fragoso@urv.cat

Featured Application: Electrochemical detection of phenoxy herbicides based on peroxidase inhibition using a carbon nano-onion modified biosensor.

Abstract: Carbon nano-onions are emerging electrode materials in biosensing due to their high conductivity and biocompatibility. Phenoxy-based herbicides are a source of environmental contamination that can be detected using their property to inhibit the activity of some enzymes. Here we report a biosensor based on peroxidase immobilized on carbon nano-onions in a cyclodextrin polymer matrix for the amperometric detection of 2,4-D and 2,4,5-T. The inhibition mechanism of 2,4-D and 2,4,5-T on peroxidase activity was first elucidated by activity measurements and molecular docking. The biosensor was characterized by electrochemical and microscopy methods and applied to the amperometric detection of these herbicides. The incorporation of carbon nano-onions enhanced the sensitivity of the biosensor and improved its stability and repeatability. The application of the developed biosensor to the detection of 2,4-D in soil and 2,4,5-T in river water samples is also reported.

Keywords: carbon nano-onion; peroxidase; phenoxy herbicide; 2,4-D; 2,4,5-T; electrochemical biosensor; cyclodextrin

Citation: Sok, V.; Fragoso, A. Carbon Nano-Onion Peroxidase Composite Biosensor for Electrochemical Detection of 2,4-D and 2,4,5-T. *Appl. Sci.* **2021**, *11*, 6889. https://doi.org/10.3390/app11156889

Academic Editor: Gang Wei

Received: 14 July 2021
Accepted: 26 July 2021
Published: 27 July 2021

1. Introduction

Carbon nanomaterials emerged as one of the most suitable materials in biosensing due to a combination of chemical versatility and electronic properties [1]. In particular, carbon nano-onions (CNOs) were recently revealed as suitable electrode materials for the detection of small molecules [2,3], antibodies [4] and glyphosate [5]. CNOs are formed by concentric graphitic layers with increasing diameters and possess a distinctive combination of high conductivity and biocompatibility, among other interesting properties [6]. They can be easily modified by a wide range of functional groups and incorporated in composite materials with organic or inorganic polymers for a wide range of applications, including energy storage [7] and biomedicine [8], among others.

Phenoxy herbicides, such as 2,4-dichlorophenoxyacetic acid (2,4-D) and 2,4,5-trichlorophenoxyacetic acid (2,4,5-T), are synthetic analogs of auxin plant growth hormones derived from phenoxyacetic acid [9]. They were successfully used to control broad-leaved weeds in several crops, as well as in forestry, urban parks and domestic gardens but are also considered a source of environmental contamination of soil and groundwater with potential carcinogenic effects in humans [10]. Hence, sensitive detection methods were developed for monitoring these herbicides. These include, but are not limited to, chromatography and immunoassays, which often need to be combined with extraction methods to guarantee their isolation and enrichment in complex samples such as soil [11].

Enzymatic biosensors based on enzyme activity inhibition were developed for pesticide detection as an alternative to traditional methods due to their simplicity and reusability [12,13]. There are only a few reports on the use of this strategy to detect phenoxy herbicides. In an early work, the inhibitory effect of 2,4-D and 2,4,5-T on the activity of

cholinesterase was used to develop an amperometric biosensor based on the use of antibodies in solution or immobilized in nitrocellulose membranes [14]. Alkaline phosphatase (ALP) immobilized on sol-gel/chitosan film on carbon paste electrodes was used to detect these herbicides in the presence of heavy metals based on the inhibition of ascorbic acid 2-phosphate hydrolysis [15]. More recently, Lui et al. reported the inhibition mechanism of 2,4-D to catalase supported on porous calcium phosphate and the construction of a biosensor based on a flow-injection analysis system to detect 2,4-D in commercial bean sprouts samples [16].

Horseradish peroxidase (HRP, EC 1.11.1.7) is a heme-containing metalloenzyme that utilizes peroxides such as hydrogen peroxide to oxidize a wide variety of organic and inorganic compounds. It is perhaps the most used enzyme in bioanalysis due to its high stability, ease of conjugation, low price compared to other widespread alternatives such as ALP and high turnover rate that allows the generation of strong signals in a relatively short time [17]. Its inhibition was only applied to detect glyphosate and its metabolites [18,19] with very little application to other herbicides [20].

Herein we report the inhibition mechanism of 2,4-D and 2,4,5-T on HRP activity and the development of an amperometric biosensor for the detection of these herbicides in soil and river water samples. HRP was conjugated to activated CNOs and immobilized on the surface of screen-printed carbon electrodes (SPE) using a β-cyclodextrin polymer as a cross-linker. Detection is based on the inhibition of HRP activity, which, to the best of our knowledge, has not been used for the detection of this family of herbicides. The effect of the CNOs on the analytical parameters and biosensor stability was also studied.

2. Materials and Methods

2.1. Materials and Reagents

All chemicals and solvents were used as received. Oxidized CNOs were prepared by oxidation of CNOs (100 mg) with 10 mL of HNO_3/H_2SO_4 (1:3 v/v) for one hour at room temperature [21]. 2,4-D, 2,4,5-T, phosphate-buffered saline (PBS), maleimide activated peroxidase from horseradish (M-HRP, 200 units mg^{-1}) and 3,3′,5,5′-tetramethylbenzidine (TMB) Liquid Substrate System for ELISA were purchased from Merck. Screen-printed electrodes (DRP-110) were obtained from Metrohm DropSens. All solutions were prepared with water purified using a Milli-Q water purification system (Millipore, Burlington, MA, USA) to a resistivity of 18.2 MΩ·cm.

2.2. Immobilization of M-HRP and Inhibition Assays

Cyclodextrin-modified Reacti-Bind™ Maleimide Activated Plates (8-well strips) were prepared as described previously [22]. M-HRP peroxidase (0.1 mg/mL in PBS buffer pH 6.0) was immobilized on the coated plates for 3 h at 4 °C. After recovering the excess of M-HRP solution, the wells were washed with PBS Tween 4 times and stored in the fridge when not in use. The activity of immobilized HRP was measured at 650 nm using TMB Liquid Substrate System for ELISA as a substrate on a SpectraMax 340PC Microplate Reader on 96-well microplates at 25 °C. All measurements were performed in 4 replicates in 0.01 M phosphate buffer pH 6.5 containing 0.138 M NaCl and 0.0027 M KCl. The Michaelis–Menten constant (K_m) and maximal velocity (V_{max}) of each herbicide were determined through Lineweaver–Burk plot analysis using various concentrations of H_2O_2 (0.0225–0.05 mM in 0.08 mM TMB) as substrate. The inhibition constants (K_I, K_{IS}) were determined from the slope of the linear dependence of the slopes and intercepts, respectively, of the Lineweaver–Burk plots versus pesticide concentration [5].

2.3. Computational Docking Study

The docking study was carried out as previously reported [23]. The HRP/herbicide structures were simulated using the crystal structure of HRP from *Armoracia rusticana* (PDB ID: 1HCH) as pdb file. 2,4,5-T and 2,4-D (deprotonated forms) were first energy-minimized at the PM3 level using Hyperchem 7.0 and used as ligand input structures for docking. The

HRP/herbicide structure and interactions were visualized using BIOVIA Discovery Studio 2017 (Accelrys).

2.4. Synthesis of Thiolated Cyclodextrin Polymer (ACDPSH)

One gram of epichorohydrin cross-linked β-cyclodextrin [24] was dissolved in 25% tetramethylammonium hydroxide (5 mL) and acetylated with 1-acetylimidazole (1 g) for 2 h at room temperature [25]. The reaction mixture was neutralized with 6 M HCl, and the precipitate of acetylated cyclodextrin polymer was collected by centrifugation, washed with water and vacuum dried over P_4O_{10} (0.9 g). Thiol groups were introduced on this polymer as reported before [24] to give a thiolated cyclodextrin polymer (ACDPSH, 0.43 g) as an off-white solid. This material contains an average of 3.3 OAc and 1.3 $HN(CH_2)_2SH$ groups per cyclodextrin unit according to ^{1}H-NMR in D_2O and dissolves in water and buffers below pH 5.5.

2.5. Biosensor Preparation and Herbicide Detection

The coating solution of the working electrode was prepared as follows: 0.5 mg of ox-CNO was mixed with 1 mg EDC and 2 mg NHS in 500 µL acetate buffer pH 5 and stirred at 4 °C for 1 h, followed by the addition of 2 mg of cystamine free base. The mixture was stirred for another 2 h at 4 °C, centrifuged and washed with water. The solid was resuspended in 500 µL of 0.1 M PBS pH 7.2 containing 0.5 mg $NaCNBH_3$, sonicated for 5 min, and 1 mg of M-HRP was added. After 4 h at room temperature, the CNO/HRP conjugate was filtered through a 100 kDa Amicon® centrifugal filter to remove the excess of M-HRP, and the retentate (~160 µL) was mixed with 200 µL of a 10% ACDPSH suspension in PBS buffer pH 6.0. A clear solution was obtained after stirring overnight at room temperature, and 3 µL of this solution were dropped on the surface of the SPEs and dried under vacuum for 2 h (SPE/CD/CNO/HRP electrodes).

Control electrodes (SPE/CD/HRP) were prepared in a similar way but without CNOs. 0.5 mg of maleimide-activated HRP were mixed with 200 µL of 10% CDPSH suspension in PBS buffer pH 6.0 and stirred overnight at room temperature to obtain a clear solution. The activity of the conjugate was measured spectrophotometrically in order to ensure that both types of electrodes contained the same amount of immobilized HRP. Finally, 2.2 µL of this solution were dropped on the surface of the SPEs and dried under vacuum for 2 h (SPE/CD/HRP). The electrodes were stored in 20 mM PBS pH 7 in the fridge when not in use.

Cyclic voltammetry (CV) and direct current (DC) amperometric measurements were carried out on an Autolab model PGSTAT 10 potentiostat/galvanostat controlled with GPES software (Eco Chemie, the Netherlands) in stirred electrolytes (425 rpm) at an applied potential of 0.0 V (vs. Ag/AgCl) in PBS pH 6. According to CV, at this potential, the electrochemical reduction of the enzyme-oxidized substrates takes place (see below). With the responses of the biosensors, the corresponding calibration curves were built by measuring the inhibition percent of HRP response in the presence of increasing concentrations of the herbicides. The SPE/CD/CNO/HRP biosensor was used to detect 2,4-D in soil. The soil sample (previously dried at 50 °C overnight) was homogenized manually, and 2,4-D was extracted by treating 1 g of solid with 2 × 10 mL of methanol for 2 h. After centrifugation at 5000 rpm for 10 min, the methanol extract was isolated and evaporated, and the residue was dissolved in 2 mL of 0.1 mM NaOH to dissolve the herbicide. The pH was adjusted to 7 with HCl 6 M, and the aqueous sample was analyzed as described before. The extractions were performed in triplicate, and the results were compared with those obtained using an ELISA kit (Abnova) following the instructions of the manufacturer. 2,4,5-T was detected in spiked samples of water collected from the Francolí river (Tarragona city). The sample was collected at the coordinates 41°07′12.0″ N+1°14′07.8″ E and filtered using a syringe filter (0.22 µm) before spiking with 3 µM 2,4,5-T.

The stability of the biosensors stored in the fridge in PBS at 4 °C was studied for 40 days by measuring the inhibition of enzyme activity of 3 µM 2,4,5-T in 4-day intervals.

Repeatability (repeated measurements on a single electrode) was studied on three identical electrodes until the signal decreased by 10% with respect to the original signal for the above concentration.

3. Results and Discussion

3.1. Inhibition Mechanism of 2,4-D and 2,4,5-T on the Activity of HRP

The determination of the inhibition mechanism is an important step in the design of sensors based on the inhibition of enzyme activity. The dependence of the enzymatic activity versus HRP concentration in the presence of increasing concentrations of the herbicides is presented in Figure 1a,b. The obtained family of straight lines with intercepts essentially equal to zero indicate a reversible inhibition since increasing inhibitor concentrations provoked a decrease in the slopes of the lines.

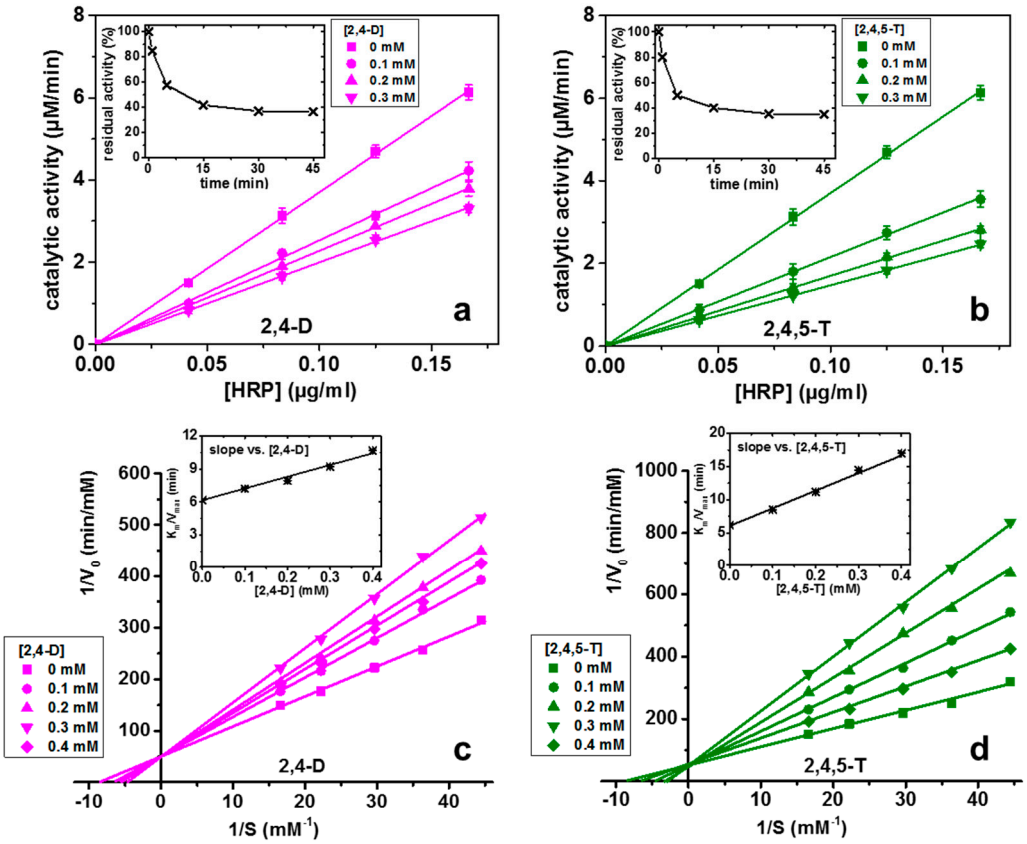

Figure 1. Top: Effect of 2,4-D (**a**) and 2,4,5-T (**b**) on the activity of HRP at different enzyme concentrations. Inset: Residual activity vs. time plots. Bottom: Lineweaver–Burk plots for the inhibition of 2,4-D (**c**) and 2,4,5-T (**d**) on the activity of immobilized HRP at different concentrations of pesticide. Inset: Secondary plots (slope vs. concentration and intercept vs. concentration) used for the determination of inhibition constants. Conditions: 10 mM phosphate-buffered saline pH 6.5, 25 °C.

Since in our sensor HRP is part of a composite deposited on the electrode surface, we also studied the inhibition of HRP immobilized on maleimide plates using a thiolated cyclodextrin polymer as a cross-linker. The maximum enzyme activity inhibition (~60%) was attained after 15 min of the interaction of the herbicides with immobilized HRP (Figure 1a,b, inset). The kinetic behavior of HRP in the presence of 2,4-D and 2,4,5-T was also studied using the Michaelis–Menten formalism by constructing double-reciprocal Lineweaver–Burk plots (Figure 1c,d). As can be seen, both herbicides gave a family of straight lines with different slopes and the same intercept located on the $1/V_0$ (vertical) axis, indicating a competitive inhibition. This means that they are bound to the free enzyme but not to the enzyme-substrate complex. This results in an increase of K_m of HRP without

changing V_{max}. The inhibitor constant (K_I) for the binding of these herbicides with the enzyme was estimated from the slope of the apparent Michaelis–Menten constant ($K_{m\ app}$) versus inhibitor concentration to be (210 ± 20) and (560 ± 40) μM for 2,4,5-T and 2,4-D, respectively (Figure 1c,d, inset).

To further understand the inhibition mechanism of HRP by 2,4-D and 2,4,5-T, their docking geometries were examined based on the X-ray crystal structure of HRP (PDB code 1HCH) and fully deprotonated ligands (Figure 2). In both cases, the ligand is oriented with the carboxylate group pointing toward the inside of the cavity interacting with guanidine residue of Arg-38. The interactions are stabilized by a set of hydrophobic and π interactions. In 2,4-D (Figure 2a), the 2-Cl atom interacts with Leu-138 via π-π interaction, while the 4-Cl atom and the aromatic ring of Phe-68 form a halogen-π bridge. There is also a favorable π-σ interaction between the aromatic ring of 2,4-D and Ala-140, and the 4-Cl atom is exposed to the solvent (Figure 2b). Meanwhile, 2,4,5-T has a more complex interaction pattern with the active site of HRP (Figure 2c). The hydrophobic interaction involving the 4-Cl atom is similar to 2,4-D, but the interactions involving the other two chlorine atoms are different, with the 2-Cl atom halogen bound simultaneously to Phe-142 and Phe-179 and the 5-Cl atom to Leu-138, resulting in 2,4,5-T being rotated ~180° as compared to 2,4-D. This more complex interaction pattern results in a deeper penetration in the active site (compare lateral views in Figure 2b,d) and is consistent with the lower K_I of 2,4,5-T with respect to 2,4-D. This means that a lower concentration of 2,4,5-T is required to produce half-maximum inhibition.

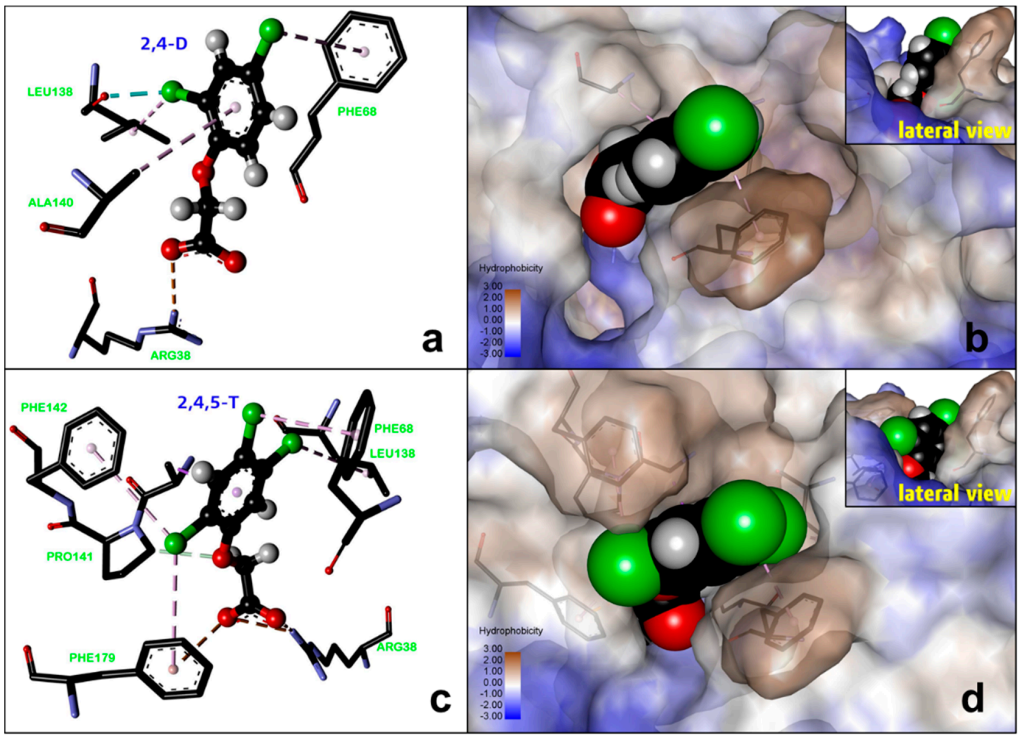

Figure 2. Left: Calculated 3D structure for the interaction of 2,4-D (**a**) and 2,4,5-T (**c**) with the active site of HRP. **Right:** Tertiary structure of HRP with 2,4-D (**b**) and 2,4,5-T (**d**) bound to the active site. Inset: lateral view (rotated ~90° from the above).

3.2. Characterization of Modified Electrodes

Cyclodextrins possess the remarkable property to form inclusion complexes with a wide variety of hydrophobic guests [26]. Modified and polymeric CDs were widely used as a platform for enzyme immobilization [27] and electrode modification in biosensors [28], so we hypothesized that the combination of inclusion ability and immobilization platform might be beneficial in the construction of a biosensor for 2,4-D and 2,4,5-T based on inhibi-

tion of the enzymatic activity of HRP (Figure 3). To prepare the biosensor, a CNO/HRP conjugate was first prepared by covalent attachment of maleimide activated HRP to the carboxylic acid groups of ox-CNO previously modified with cysteamine. This conjugate contained an average of three HRP molecules per CNO as determined by atomic absorption spectroscopy [29] and was further cross-linked with a thiolated CD polymer to form a coating composite.

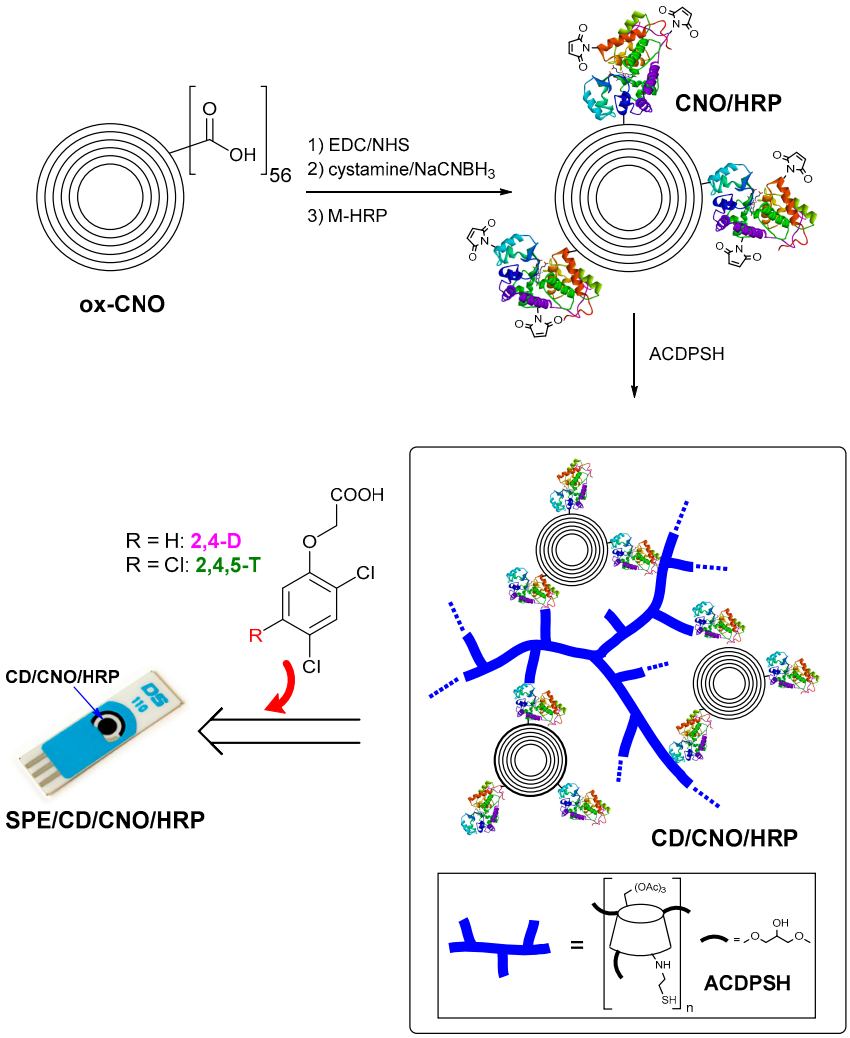

Figure 3. Preparation of SPE/CD/CNO/HRP electrodes.

Figure 4a shows an HRTEM image of the starting CNOs obtained from nanodiamond annealing in which the multilayered graphitic structure is clearly visible. TEM images of a thin film of the CD/CNO/HRP conjugate show a network-like distribution of the CNO/HRP aggregate nanoparticles in the organic polymer matrix (Figure 4b). The CD/CNO/HRP composite completely covers the electrode surface forming a thin film of ~2 µm thickness. The surface shows a markedly rough and filamented morphology as compared with the bare electrode due to the presence of the CNO/HRP conjugate (Figure 4c,d) as revealed by ESEM analysis.

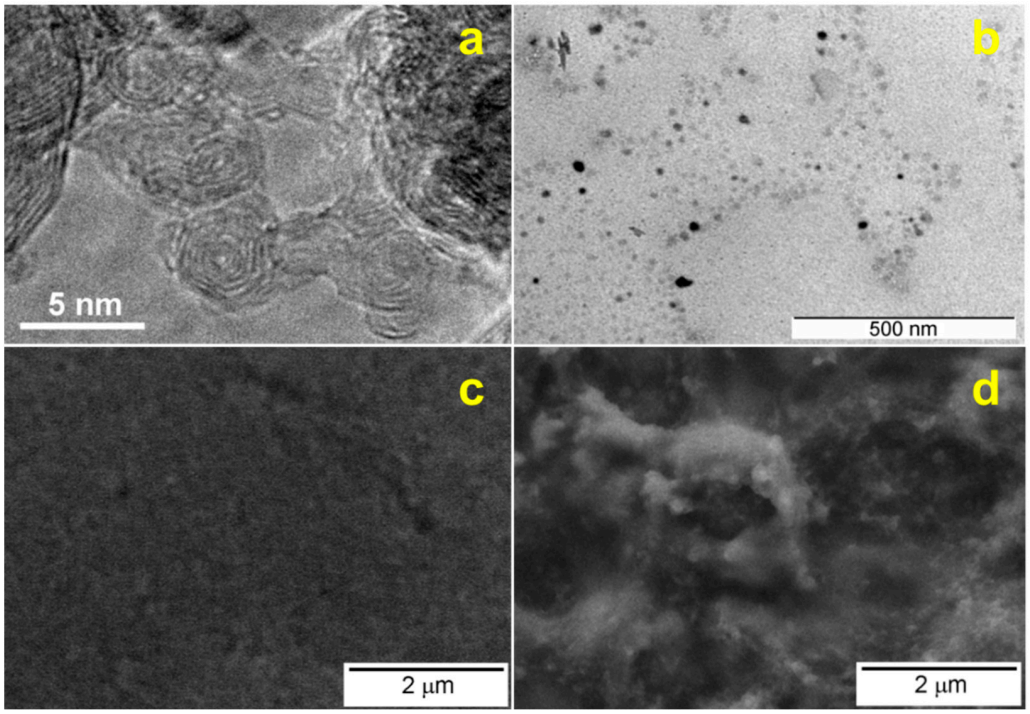

Figure 4. (**a**) HRTEM image of the starting CNOs. (**b**) TEM image of the CD/CNO/HRP composite before deposition on the SPEs. (**c**) ESEM image of the bare SPE and (**d**) SPE/CD/CNO/HRP.

Figure 5a shows the cyclic voltammograms (CV) of bare SPE, SPE/CD/CNO/HRP and a control sensor without CNO (SPE/CD/HRP) using $Fe[(CN)_6]^{3-}$ in KCl as an electroactive marker. SPE/CD/CNO/HRP showed a notably higher peak current signal as compared to SPE/CD/HRP and SPE. The electroactive area of the electrodes accessible to the redox probe was determined using the Randles-Ševčík equation: $i_p = 2.69 \times 10^5 D^{1/2} n^{3/2} v^{1/2} Ac$, where i_p is the peak current (A), D is the diffusion coefficient of $Fe[(CN)_6]^{3-}$ in aqueous solution (7.3×10^{-6} cm^2 s^{-1}) [30], n is the number of transferred electrons by $Fe[(CN)_6]^{3-}$ ($n = 1$), v is the scan rate (V s^{-1}), A is the electroactive surface (cm^2) and c is the concentration of the marker (mol cm^{-3}). Based on this equation, by plotting the values of i_p versus $v^{1/2}$, the calculated electroactive surface of were (0.69 ± 0.03) cm^2, (0.59 ± 0.04) and (0.51 ± 0.01) cm^2 for SPE/CD/CNO/HRP, SPE/CD/HRP and SPE, respectively, which indicate that the composites deposited on SPE significantly increased their surface area. The presence of CNO also increased the peak current by 42% in comparison to SPE/CD/HRP and decreased the peak-to-peak separation from 183 mV in the SPE/CD/HRP electrode to 149 mV in SPE/CD/CNO/HRP. This indicates that the CNOs also play an important role in the composite by facilitating electron transfer across the solution/electrode interface.

Figure 5b shows the CVs of bare and modified electrodes using TMB in PBS as an electroactive marker. In all cases, two current peaks appear in both oxidation and reduction sweeps, corresponding to the exchange of one electron in each case. At the bare electrode, these pairs of peaks are well resolved, while in the modified electrodes, the peaks are broad, and their intensity decreases in the order SPE/CD/CNO/HRP > SPE/CD/HRP > SPE, similar to what was observed for $Fe[(CN)_6]^{3-}$. The peak potentials in the reduction sweep are displaced to more positive potentials, making the redox process more reversible. All these features indicate that the SPE/CD/CNO/HRP composite is permeable to the enzyme substrate, and its electroactive properties are favored with respect to the bare electrode, presumably due to an interfacial accumulation mechanism [31].

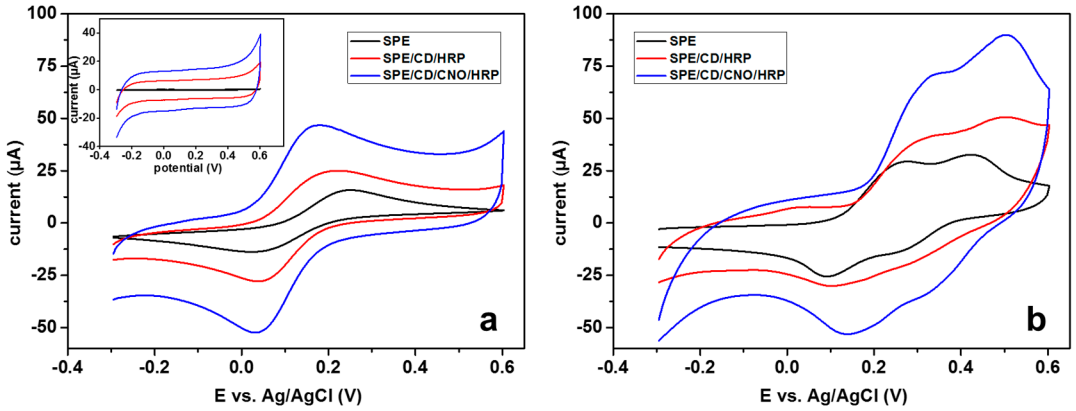

Figure 5. Cyclic voltammograms of 0.1 M KCl (**a**, **inset**), 1 mM $K_3[Fe(CN)_6]$ in 0.1 M KCl (**a**) and 0.5 mM TMB hydrochloride in 0.1 M PBS pH 6.5 (**b**). Scan rate: 100 mV/s.

3.3. Amperometric Detection of 2,4-D and 2,4,5-T

As shown above, 2,4-D and 2,4,5-T behave as reversible competitive inhibitors; hence by measuring the amperometric response of the biosensors at increasing concentrations of the herbicides, it was possible to construct calibration plots (% inhibition vs. concentration) for both of them and estimate the analytical parameters based on a two-step assay protocol (Scheme 1a).

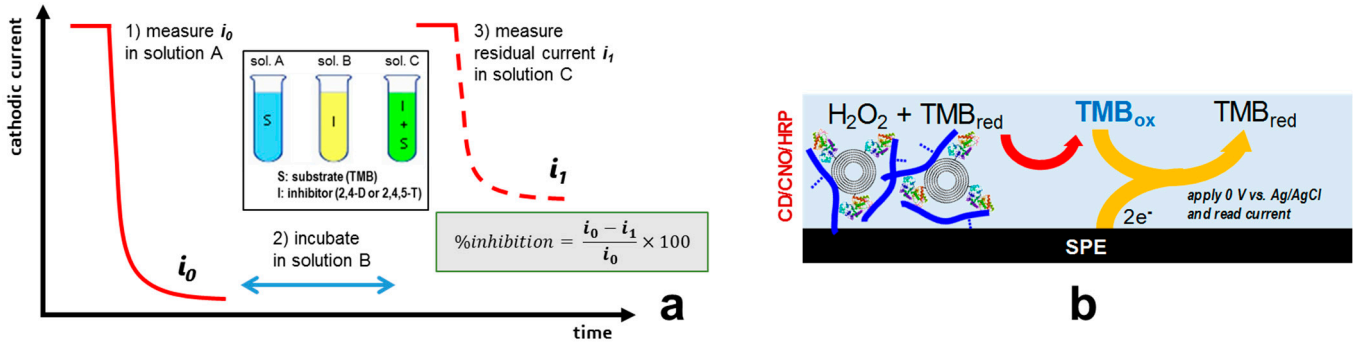

Scheme 1. (**a**) Inhibition measurements based on a two-step assay procedure. (**b**) Amperometric detection mechanism.

To reach the highest sensitivity, various conditions such as substrate concentrations and incubation times were first optimized. These steps are necessary due to the heterogeneous nature of the biosensor interface given by the active membrane that has a finite permeability to ions and reagents. For this, the biosensors were incubated with the substrate for a given time, and the reduction current due to oxidized TMB was measured at a fixed potential (Scheme 1b). Hence, an important parameter to optimize in this type of system is the time the biosensors are kept in contact with the inhibitors (step 2 in Scheme 1a). In reversible competitive inhibition, the inhibitor and substrate compete for the active site of the enzyme, and for a constant substrate concentration, the activity decreases with increasing inhibitor concentration. In our case, this interaction requires some time to stabilize due to the heterogeneity of the thin film containing the enzyme, and, as seen in Figure 6a, the current decrease with respect to the non-inhibited system reached a maximum after 3 min of exposure to the herbicides. Another important parameter is the time needed to attain the maximum current response in steps 1 and 3 of Scheme 1a. Figure 6b shows the current progress vs. time of SPE/CD/CNO/HRP with and without the presence of a fixed concentration of the herbicides. As seen in the figure, the steady-state current is reached between 50 and 60 s after exposing the biosensors to the substrate solution, and the current response remained stable for several minutes. Hence, after measuring the initial substrate signal (step 1 in Scheme 1a), the biosensors were incubated for 3 min with the

herbicide (step 2 in Scheme 1a) before reading the amperometric signal for ~ 1 min (step 3 in Scheme 1a).

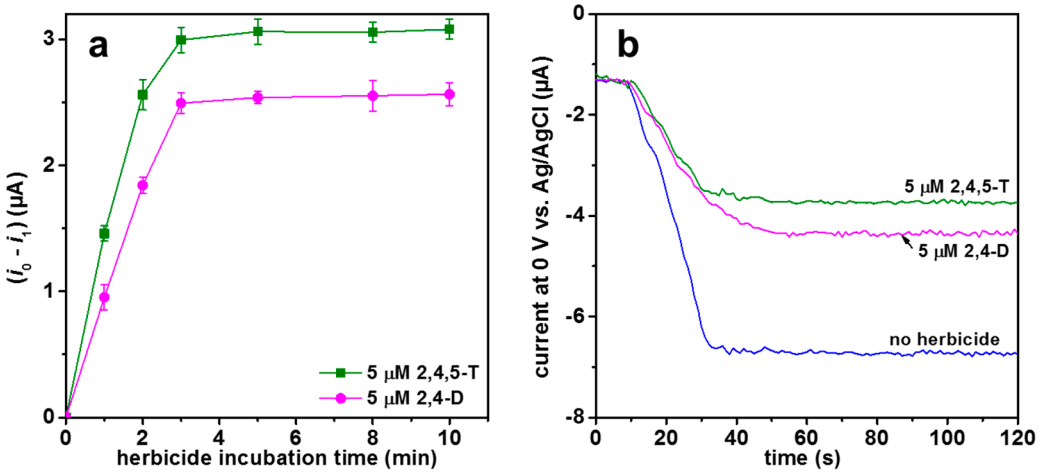

Figure 6. Current variation at different incubation times (**a**) and chronoamperometric responses (**b**) of SPE/CD/CNO/HRP in the presence of the herbicides in 10 mM PBS, pH 6.5.

The ability of many toxic substances to inhibit the catalytic activity of enzymes has contributed to the development of biosensors for the detection and quantification of pollutants such as herbicides and pesticides in general [13]. The relative inhibition of enzyme activity was correlated with the herbicide concentration by measuring the decrease in amperometric response of the biosensors in the absence and presence of 2,4-D and 2,4,5-T using the optimized conditions described above. Figure 7 shows the calibration curves of 2,4-D and 2,4,5-T for SPE/CD/CNO/HRP and control SPE/CD/HRP biosensors. The inhibition percent initially increases almost linearly with pesticide concentration then tends slowly to saturation, with a maximum inhibition percent of 44% for 2,4-D and 55% for 2,4,5-T. Table 1 shows the analytical parameters for the biosensors assuming a linear relationship below 1 μM. In the CNO-containing biosensor, the sensitivity was higher, and the LOD was lower than those obtained with the SPE/CD/HRP biosensors, similar to what was previously observed with other CNO-based transducer surfaces [2,4,5] and due to the enhancement of electron transfer provided by the CNO-nanoparticles. It should also be noted that the LODs obtained (<10 μg/L) are well below the maximum contaminant level of 0.07 and 0.05 mg/L allowed in the United States for 2,4-D and 2,4,5-T herbicides and the value recommended by the World Health Organization for 2,4-D (30 μg/L). To the best of our knowledge, this is the first example of an HRP-based biosensor for phenoxy herbicides detection, which is more sensitive in comparison to other developed biosensors (Table 2).

Table 1. Analytical parameters of the developed biosensors.

Sensor	Herbicide	Sensitivity (μM^{-1})	LOD (nM)	LOD (μg/L)
SPE/CD/CNO/HRP	2,4-D	17 ± 2	23 ± 3	5.1
SPE/CD/HRP	2,4-D	5.4 ± 0.6	33 ± 4	7.3
SPE/CD/CNO/HRP	2,4,5-T	22 ± 2	10 ± 3	2.6
SPE/CD/HRP	2,4,5-T	8.5 ± 0.7	17 ± 2	4.4

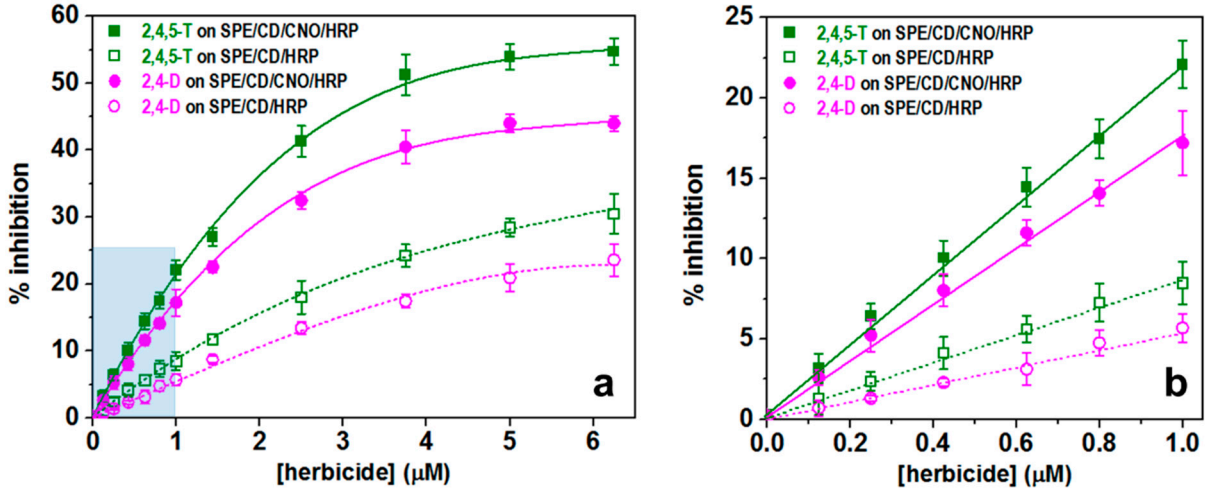

Figure 7. (**a**) Calibration curves of 2,4-D and 2,4,5-T obtained on SPE/CD/CNO/HRP and SPE/CD/HRP biosensors. (**b**) Detail of the curves below 1 μM concentration and adjusted assuming a linear behavior.

Table 2. Comparison of reported detection methods for 2,4-D and 2,4,5-T.

Herbicide	Surface Chemistry	Detection Technique	Assay Time (min)	LOD (μM)	Reference
2,4-D	Catalase immobilized on porous graphene	Amperometry, enzyme inhibition	10	0.15	[16]
2,4-D	Sulfatase based whole-cell Agrobacterium biosensor	Fluorescence, enzyme activity	overnight	1.56	[32]
2,4-D	Iron (III) porphyrin on immobilized on MWCNT	Amperometry, electrocatalysis	3	2.1	[33]
2,4-D	Quantum dot modified molecule imprinting polymer	Fluorescence of nitrobenzoxadiazole	5	0.14	[34]
2,4-D	Carbon nano-onion/HRP conjugate on cyclodextrin polymer	Amperometry, enzyme inhibition	5	0.023	This work
2,4,5-T	Alkaline phosphatase/sol-gel chitosan film on carbon paste electrode	Amperometry, enzyme inhibition	15	1.9	[15]
2,4,5-T	Polyclonal antibody-based immunoassay	Colorimetric, ELISA	60	0.005	[14]
2,4,5-T	Polyclonal antibody on graphite electrode	Potentiometry, competitive assay	10	200	[35]
2,4,5-T	Albumin-2,4,5-T immobilized in membrane	Colorimetric, competitive ELISA	30	0.0028	[36]
2,4,5-T	Carbon nano-onion/HRP conjugate on cyclodextrin polymer	Amperometry, enzyme inhibition	5	0.010	This work

3.4. Stability and Repeatability of the Developed Biosensors

The long-term stability and repeatability of the biosensors were examined. Figure 8 shows the residual activities of immobilized HRP in the developed biosensors by monitoring their amperometric responses in 4-day intervals over a period of 4 weeks for electrodes stored in PBS buffer pH 6.5 at 4 °C. After the first week of storage, SPE/CD/CNO/HRP and SPE/CD/HRP maintain 97% and 85% of their initial activity, respectively, and then decreased to 77% and 58% after 4 weeks of storage. The presence of CNO covalently coupled to HRP, and the cyclodextrin matrix on the surface electrode improved the stability of SPE/CD/CNO/HRP compared to SPE/CD/HRP. This increased stability of the CNO biosensors might be attributed to Van der Waals interactions between the carbon nanoparticles and the enzyme resulting in a reduction in the enzyme mobility due to the anchorage to the support, thus shielding it from the denaturing effects of the envi-

ronment, as observed recently for HRP and other enzymes immobilized on CNOs [21]. Regarding repeatability, SPE/CD/CNO/HRP is stable for 44 measurements as compared to SPE/CD/HRP (30 measurements), taken as a signal decrease of 10%. These results can also be explained based on the stability of the enzyme composites with CNO and the presence of the polymeric matrix.

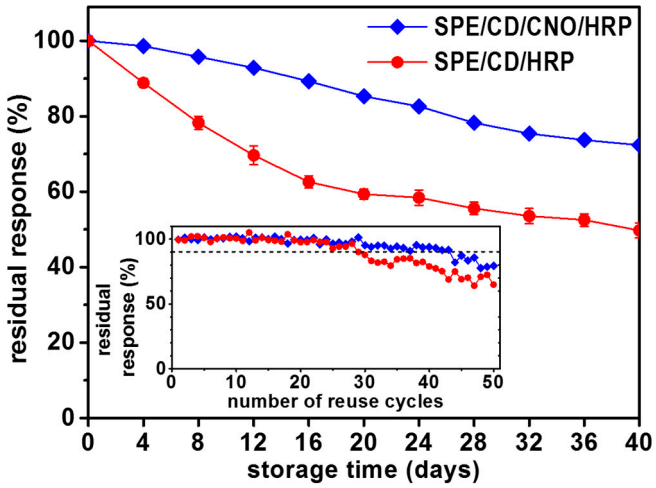

Figure 8. Storage stability and reuse cycles (inset) of SPE/CD/CNO/HRP and SPE/CD/HRP biosensors.

3.5. Analysis of Real Samples

The applicability of the biosensors in real samples was tested using soil and water samples (Table 3). 2,4-D was detected in a soil sample obtained from a local barley crop one day after the application of the herbicide. It can be seen that the concentrations obtained with the biosensor and with a commercial ELISA are in good agreement, indicating a good performance of the biosensor and similar to conventional doses used in European soils [10]. In the case of 2,4,5-T, due to the impossibility to obtain real samples contaminated with this herbicide, the CNO modified biosensor was tested in river water samples collected from the Francolí river in Tarragona and spiked with 2,4,5-T. As can be seen in Table 3, the recovery concentration obtained is 108%, demonstrating the suitability of the developed surface chemistry for detection in complex samples and could find application in agriculture to monitor the presence and environmental fate of phenoxy herbicides.

Table 3. Analysis of soil and spiked river water samples.

Herbicide	Sample	Method	Concentration
2,4-D	Soil treated with 2,4-D	SPE/CD/CNO/HRP biosensor	(11 ± 3) mg/kg
		ELISA	(9.6 ± 0.5) mg/kg
2,4,5-T	River water spiked with 2,4,5-T	SPE/CD/CNO/HRP biosensor	3.0 μM (added)
			(2.85 ± 0.05) μM (found)

4. Conclusions

We explored the possibility of using CNO-modified electrodes for the construction of an amperometric enzyme biosensor for phenoxy herbicides based on HRP immobilized on CNOs and further cross-linked with a cyclodextrin polymer. Deposition of this composite on screen-printed electrodes allowed the development of highly sensitive biosensors for 2,4-D and 2,4,5-T on soil and water samples based on the inhibition of HRP activity. The incorporation of CNOs had a positive effect in enhancing the sensitivity due to the large surface area combined with the enhanced electron transfer properties of these nanoparticles.

CNOs also proved beneficial to improve their stability and repeatability. It could thus be expected that this strategy can be further extended to develop portable pesticide detection systems for in-field agricultural or environmental applications.

Author Contributions: V.S.: investigation, data curation. A.F.: conceptualization, writing—review and editing, supervision. All authors have read and agreed to the published version of the manuscript.

Funding: This research was funded by Ministerio de Economía y Competitividad, Spain (Grant BIO2012-30936 to A.F.) and Generalitat de Catalunya (pre-doctoral scholarship 2015FI_B00523 to V.S.).

Institutional Review Board Statement: Not applicable.

Informed Consent Statement: Not applicable.

Data Availability Statement: The data presented in this study are available on request from the corresponding author.

Conflicts of Interest: The authors declare no conflict of interest.

Abbreviations

CNO	carbon nano-onion
HRP	horseradish peroxidase
2,4-D	2,4-dichlorophenoxyacetic acid
2,4,5-T	2,4,5-trichlorophenoxyacetic acid
CD	cyclodextrin
SPE	screen-printed carbon electrode
TMB	3,3′,5,5′-tetramethylbenzidine
ELISA	enzyme-linked immunosorbent assay
EDC	1-ethyl-3-(3-dimethylaminopropyl)carbodiimide
NHS	*N*-hydroxysuccinimide

References

1. Speranza, G. Carbon nanomaterials: Synthesis, functionalization and sensing applications. *Nanomaterials* **2021**, *11*, 967. [CrossRef]
2. Bartolome, J.P.; Fragoso, A. Electrochemical detection of nitrite and ascorbic acid at glassy carbon electrodes modified with carbon nano-onions bearing electroactive moieties. *Inorg. Chim. Acta* **2017**, *468*, 223–231. [CrossRef]
3. Sohouli, E.; Keihan, A.H.; Shahdost-Fard, F.; Naghian, E.; Plonska-Brzezinska, M.E.; Rahimi-Nasrabadi, M.; Ahmadi, F. A glassy carbon electrode modified with carbon nanoonions for electrochemical determination of fentanyl. *Mat. Sci. Eng. C* **2020**, *110*, 110684. [CrossRef] [PubMed]
4. Zuaznabar-Gardona, J.C.; Fragoso, A. Development of highly sensitive IgA immunosensors based on co-electropolymerized L-DOPA/dopamine carbon nano-onion modified electrodes. *Biosens. Bioelectron.* **2019**, *141*, 111357. [CrossRef]
5. Sok, V.; Fragoso, A. Amperometric biosensor for glyphosate based on the inhibition of tyrosinase conjugated to carbon nano-onions in a chitosan matrix on a screen-printed electrode. *Microchim. Acta* **2019**, *186*, 569. [CrossRef] [PubMed]
6. Mykhailiv, O.; Zubyk, H.; Plonska-Brzezinska, M.E. Carbon nano-onions: Unique carbon nanostructures with fascinating properties and their potential applications. *Inorg. Chim. Acta* **2017**, *468*, 49–66. [CrossRef]
7. Plonska-Brzezinska, M.E. Carbon nano-onions: A review of recent progress in synthesis and applications. *ChemNanoMat* **2019**, *5*, 568–580. [CrossRef]
8. Bartkowski, M.; Giordani, S. Carbon nano-onions as potential nanocarriers for drug delivery. *Dalton Trans.* **2021**, *50*, 2300–2309. [CrossRef] [PubMed]
9. Magnoli, K.; Carranza, C.S.; Aluffi, M.E. Herbicides based on 2,4-D: Its behavior in agricultural environments and microbial biodegradation aspects. A review. *Environ. Sci. Pollut. Res.* **2020**, *27*, 38501–38512. [CrossRef]
10. Boivin, A.; Amellal, S.; Schiavon, M.; van Genuchten, M.T. 2,4-Dichlorophenoxyacetic acid (2,4-D) sorption and degradation dynamics in three agricultural soils. *Environ. Pollut.* **2005**, *138*, 92–99. [CrossRef]
11. Mei, X.Y.; Hong, Y.Q.; Chen, G.H. Review on analysis methodology of phenoxy acid herbicide residues. *Food Anal. Methods* **2016**, *9*, 1532–1561. [CrossRef]
12. Karadurmus, L.; Kaya, S.I.; Ozkan, S.A. Recent advances of enzyme biosensors for pesticide detection in foods. *J. Food Meas. Charact.* **2021**, in press. [CrossRef]
13. Kurbanoglu, S.; Ozkan, S.A.; Merkoçi, A. Nanomaterials-based enzyme electrochemical biosensors operating through inhibition for biosensing applications. *Biosens. Bioelectron.* **2017**, *89*, 886–898. [CrossRef] [PubMed]

14. Medyantseva, E.; Vertlib, M.; Kutyreva, M.; Khaldeeva, E.; Budnikov, G.; Eremin, S. The specific immunochemical detection of 2,4-dichlorophenoxyacetic acid and 2,4,5-trichlorophenoxyacetic acid pesticides by amperometric cholinesterase biosensors. *Anal. Chim. Acta* **1997**, *347*, 71–78. [CrossRef]
15. Shyuan, L.; Heng, L.; Ahmad, M.; Aziz, S.; Ishak, Z. Evaluation of Pesticide and Heavy Metal Toxicity Using Immobilized Enzyme Alkaline Phosphatase with an Electrochemical Biosensor. *Asian J. Biochem.* **2008**, *3*, 359–365. [CrossRef]
16. Liu, F.; Zhong, A.; Xu, Q.; Cao, H.; Hu, X. Inhibition of 2,4-Dichlorophenoxyacetic Acid to Catalase Immobilized on Hierarchical Porous Calcium Phosphate: Kinetic Aspect and Electrochemical Biosensor Construction. *J. Phys. Chem. C* **2016**, *120*, 15966–15975. [CrossRef]
17. Veitch, N. Horseradish peroxidase: A modern view of a classic enzyme. *Phytochemistry* **2004**, *65*, 249–259. [CrossRef]
18. Songa, E.; Somerset, V.; Waryo, T.; Baker, P.; Iwuoha, E. Amperometric nanobiosensor for quantitative determination of glyphosate and glufosinate residues in corn samples. *Pure Appl. Chem.* **2009**, *81*, 123–139. [CrossRef]
19. Zhang, Q.; Xu, G.; Gong, L.; Dai, H.; Zhang, S.; Li, Y.; Lin, Y. An enzyme-assisted electrochemiluminescent biosensor developed on order mesoporous carbons substrate for ultrasensitive glyphosate sensing. *Electrochim. Acta* **2015**, *186*, 624–630. [CrossRef]
20. Moccelini, S.; Vieira, I.; de Lima, F.; Lucca, B.; Barbosa, A.; Ferreira, V. Determination of thiodicarb using a biosensor based on alfalfa sprout peroxidase immobilized in self-assembled monolayers. *Talanta* **2010**, *82*, 164–170. [CrossRef]
21. Sok, V.; Fragoso, A. Preparation and characterization of alkaline phosphatase, horseradish peroxidase, and glucose oxidase conjugates with carboxylated carbon nano-onions. *Prep. Biochem. Biotechnol.* **2018**, *48*, 136–143. [CrossRef] [PubMed]
22. Ortiz, M.; Torréns, M.; Fragoso, A.; O'Sullivan, C. Highly sensitive colorimetric enzyme-linked oligonucleotide assay based on cyclodextrin-modified polymeric surfaces. *Anal. Bioanal. Chem.* **2012**, *403*, 195–202. [CrossRef]
23. Sok, V.; Fragoso, A. Kinetic, spectroscopic and computational docking study of the inhibitory effect of the pesticides 2,4,5-T, 2,4-D and glyphosate on the diphenolase activity of mushroom tyrosinase. *Int. J. Biol. Macromol.* **2018**, *118*, 427–434. [CrossRef]
24. Fragoso, A.; Sanromà, B.; Ortiz, M.; O'Sullivan, C. Layer-by-layer self-assembly of peroxidase on gold electrodes based on complementary cyclodextrin–adamantane supramolecular interactions. *Soft Matter* **2009**, *5*, 400–406. [CrossRef]
25. Lu, Y.; Wei, P.; Pei, Y.; Xu, H.; Xin, X.; Pei, Z. Regioselective acetylation of carbohydrates and diols catalyzed by tetramethylammonium hydroxide in water. *Green Chem.* **2014**, *16*, 4510–4514. [CrossRef]
26. Szejtli, J. Introduction and General Overview of Cyclodextrin Chemistry. *Chem. Rev.* **1998**, *98*, 1743–1754. [CrossRef]
27. Villalonga, R.; Cao, R.; Fragoso, A. Supramolecular Chemistry of Cyclodextrins in Enzyme Technology. *Chem. Rev.* **2007**, *107*, 3088–3116. [CrossRef] [PubMed]
28. Ortiz, M.; Fragoso, A.; O'Sullivan, C. Detection of Antigliadin Autoantibodies in Celiac Patient Samples Using a Cyclodextrin-Based Supramolecular Biosensor. *Anal. Chem.* **2011**, *83*, 2931–2938. [CrossRef] [PubMed]
29. Visser, C.; Stevanović, S.; Voorwinden, L.; Bloois, L.; Gaillard, P.; Danhof, M.; Crommelin, D.; Boer, A. Targeting liposomes with protein drugs to the blood–brain barrier in vitro. *Eur. J. Pharm. Sci.* **2005**, *25*, 299–305. [CrossRef] [PubMed]
30. Konopka, S.; McDuffie, B. Diffusion coefficients of ferri- and ferrocyanide ions in aqueous media, using twin-electrode thin-layer electrochemistry. *Anal. Chem.* **1970**, *42*, 1741–1746. [CrossRef]
31. Zuaznabar-Gardona, J.C.; Fragoso, A. Electrochemical characterisation of the adsorption of ferrocenemethanol on carbon nano-onion modified electrodes. *J. Electroanal. Chem.* **2020**, *871*, 114314. [CrossRef]
32. Ritcharoon, B.; Sallabhan, R.; Toewiwat, N.; Mongkolsuk, S.; Loprasert, S. Detection of 2,4-dichlorophenoxyacetic acid herbicide using a FGE-sulfatase based whole-cell Agrobacterium biosensor. *J. Microbiol. Meth.* **2020**, *175*, 105997. [CrossRef] [PubMed]
33. Wong, A.; Sotomayor, M. Biomimetic sensor based on 5,10,15,20-tetrakis(pentafluorophenyl)-21H,23H-porphyrin iron (III) chloride and MWCNT for selective detection of 2,4-D. *Sens. Actuat. B* **2013**, *181*, 332–339. [CrossRef]
34. Wang, X.; Yu, J.; Wu, X.; Fu, J.; Kang, Q.; Shen, D.; Li, J.; Chen, L. A molecular imprinting-based turn-on Ratiometric fluorescence sensor for highly selective and sensitive detection of 2,4-dichlorophenoxyacetic acid (2,4-D). *Biosens. Bioelectron.* **2016**, *81*, 438–444. [CrossRef] [PubMed]
35. Dzantiev, B.; Zherdev, A.; Yulaev, M.; Sitdikov, R.; Dmitrieva, N.; Moreva, I. Electrochemical immunosensors for determination of the pesticides 2,4-dichlorophenoxyacetic and 2,4,5-tricholorophenoxyacetic acids. *Biosens. Bioelectron.* **1996**, *11*, 179–185. [CrossRef]
36. Tomassetti, M.; Martini, E.; Campanella, L. New immunosensors for 2,4-D and 2,4,5-T pesticides determination. *Int. J. Environ. Anal. Chem.* **2012**, *92*, 417–431. [CrossRef]